The Geological Society of America
Field Guide 15
2009

The Boring Volcanic Field of the Portland-Vancouver area, Oregon and Washington: Tectonically anomalous forearc volcanism in an urban setting

Russell C. Evarts
U.S. Geological Survey, 345 Middlefield Road, Menlo Park, California 94025, USA

Richard M. Conrey
GeoAnalytical Laboratory, School of Earth and Environmental Sciences, Washington State University, Pullman, Washington 99164, USA

Robert J. Fleck
Jonathan T. Hagstrum
U.S. Geological Survey, 345 Middlefield Road, Menlo Park, California 94025, USA

ABSTRACT

More than 80 small volcanoes are scattered throughout the Portland-Vancouver metropolitan area of northwestern Oregon and southwestern Washington. These volcanoes constitute the Boring Volcanic Field, which is centered in the Neogene Portland Basin and merges to the east with coeval volcanic centers of the High Cascade volcanic arc. Although the character of volcanic activity is typical of many monogenetic volcanic fields, its tectonic setting is not, being located in the forearc of the Cascadia subduction system well trenchward of the volcanic-arc axis. The history and petrology of this anomalous volcanic field have been elucidated by a comprehensive program of geologic mapping, geochemistry, $^{40}Ar/^{39}Ar$ geochronology, and paleomagnetic studies. Volcanism began at 2.6 Ma with eruption of low-K tholeiite and related lavas in the southern part of the Portland Basin. At 1.6 Ma, following a hiatus of ~0.8 m.y., similar lavas erupted a few kilometers to the north, after which volcanism became widely dispersed, compositionally variable, and more or less continuous, with an average recurrence interval of 15,000 yr. The youngest centers, 50–130 ka, are found in the northern part of the field. Boring centers are generally monogenetic and mafic but a few larger edifices, ranging from basalt to low-SiO_2 andesite, were also constructed. Low-K to high-K calc-alkaline compositions similar to those of the nearby volcanic arc dominate the field, but many centers erupted magmas that exhibit little influence of fluids derived from the subducting slab. The timing and compositional characteristics of Boring volcanism suggest a genetic relationship with late Neogene intra-arc rifting.

Evarts, R.C., Conrey, R.M., Fleck, R.J., and Hagstrum, J.T., 2009, The Boring Volcanic Field of the Portland-Vancouver area, Oregon and Washington: Tectonically anomalous forearc volcanism in an urban setting, *in* O'Connor, J.E., Dorsey, R.J., and Madin, I.P., eds., Volcanoes to Vineyards: Geologic Field Trips through the Dynamic Landscape of the Pacific Northwest: Geological Society of America Field Guide 15, p. 253–270, doi: 10.1130/2009.fld015(13).

INTRODUCTION

The Boring Volcanic Field is an assemblage of late Pliocene and Pleistocene volcanic vents and associated lava flows dispersed throughout the greater Portland-Vancouver metropolitan area of northwestern Oregon and southwestern Washington (Fig. 1). The name derives from a group of volcanic-capped hills near the community of Boring, ~20 km southeast of downtown Portland (Treasher, 1942a, 1942b). The limits of the volcanic field are well defined except on the east where it merges into coeval volcanic rocks of the Cascade volcanic arc (Peck et al., 1964); following Allen (1975) and Tolan and Beeson (1984), we arbitrarily place the eastern boundary of the Boring Volcanic Field at longitude 122°W. The area of the field so defined is

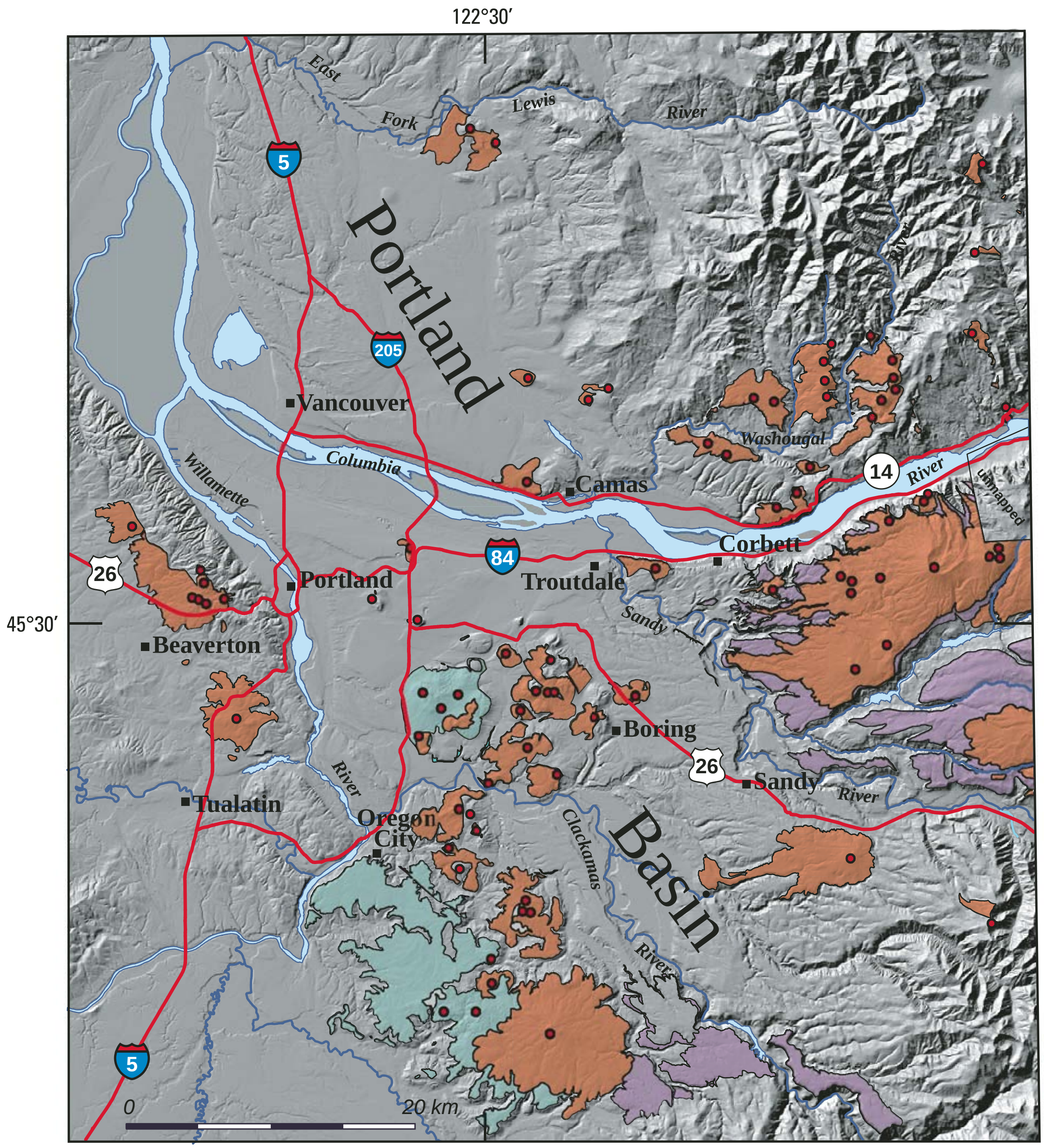

Figure 1. Boring Volcanic Field and Portland Basin on hillshade image derived from 30-m digital elevation model, showing locally erupted volcanic rocks (in orange except for low-K tholeiites in blue), vents (red circles), and low-K tholeiites of High Cascades (purple).

~4000 km^2, of which ~500 km^2 is underlain by locally erupted volcanic rocks with a total volume near 10 km^3. Boring Volcanic Field volcanism, like that of the Cascade arc, is apparently related to subduction of the Juan de Fuca oceanic plate beneath western North America. However, the tectonic position of the field is anomalous, being located in the forearc of the Cascadia convergent margin well trenchward of the volcanic arc defined by large, long-lived stratovolcanoes such as Mount Hood and Mount St. Helens (Hildreth, 2007; Fig. 2). Vents in the field are found as far as 90 km west of the arc axis near Mount Hood.

The existence of geologically young volcanic rocks within the Portland metropolitan area has been recognized for over a century (Williams, 1916). Yet despite the obvious hazards and neotectonic implications of young volcanism in an urban setting, surprising little was known of the age and composition of Boring volcanoes until recently. In his mapping of the Portland area, Trimble (1963) showed the distribution of Boring volcanics as a single map unit although he recognized that they were products of multiple vents. In a short paper, Allen (1975) inferred the locations of dozens of presumed Boring vents largely on geomorphic grounds. Hammond (1980), Hammond and Korosec (1983), Madin (1994), and Barnes (1995) were the first to distinguish among Boring flows based on their geochemistry and mapped vent locations and to employ isotopic dating to ascertain their ages. More recently, Conrey et al. (1996a, 1996b) published K-Ar dates for several dozen young volcanic centers in the region between Portland and Mount Hood.

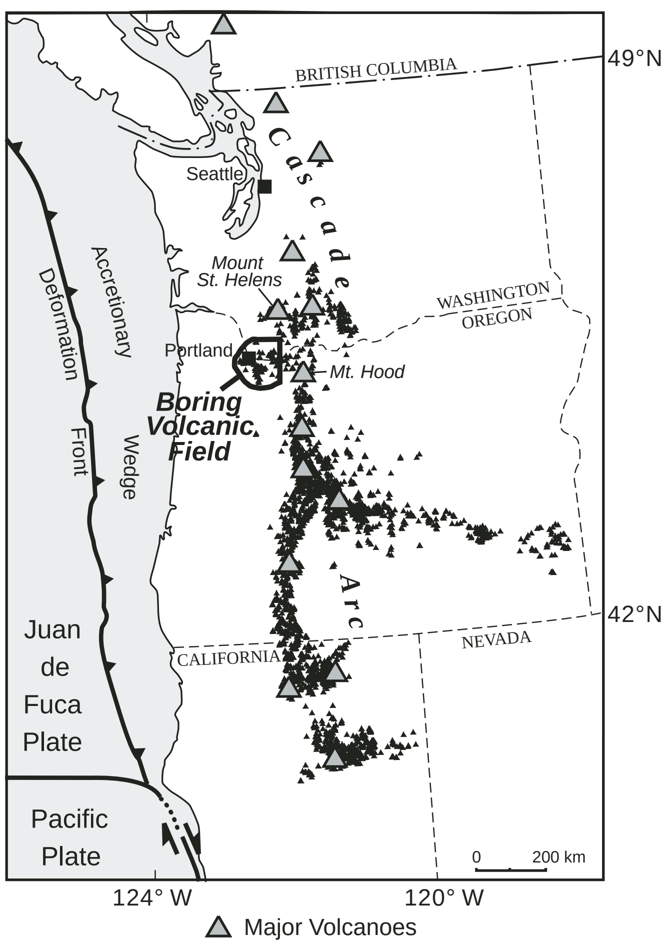

Figure 2. Regional tectonic and volcanic setting of the Boring Volcanic Field. Volcanic vents in the Pacific Northwest younger than 5 Ma from Guffanti and Weaver (1988).

In order to fully characterize the Boring Volcanic Field and assess its neotectonic and hazards significance, we have undertaken an integrated program of geologic mapping, petrographic and geochemical analyses, $^{40}Ar/^{39}Ar$ dating, and paleomagnetic determinations in an attempt to document every center in the field. Most of the area has been mapped at 1:24,000 scale except for the easternmost part of the field, where coverage is incomplete. The work reported here takes advantage of the capability for the rapid and precise determination of chemical composition possible with modern automated X-ray fluorescence spectrometry (XRF) instrumentation and the more precise geochronological data obtainable with $^{40}Ar/^{39}Ar$ dating. The $^{40}Ar/^{39}Ar$ technique is particularly valuable because it allows recognition of disturbed systematics owing to weathering or the presence of excess or inherited argon, which can result in erroneous conventional K-Ar ages. We have also acquired laboratory paleomagnetic data for Boring lava flows and intrusions, which provide a consistency test for the radiometric ages and can be used to correlate dispersed outcrops.

GEOLOGIC SETTING

The Boring Volcanic Field extends from the Cascade Range westward across the southern part of the Portland Basin, a late Neogene to Quaternary topographic and structural depression within the Puget-Willamette forearc trough of the Cascadia subduction system (Fig. 2). The shallow (<600 m deep) basin is superimposed on the Paleogene strandline that separates subaerial volcanic rocks of the western Cascade Range to the east from coeval marine sedimentary rocks to the west. A proto–Portland Basin began to form ca. 17 Ma, coincident with the arrival of early flood-basalt flows of the Columbia River Basalt Group. The Columbia River has traversed the basin since its inception and delivered most of the sediment that now fills it. The older part of this fill, predating Boring volcanism, constitutes the late Miocene and Pliocene Sandy River Mudstone and Troutdale Formation (Trimble, 1963). These units consist largely of fine-grained micaceous, arkosic sandstone and cobbly conglomerate that contains clasts of Columbia River Basalt as well as quartzite and other rock types eroded from pre-Tertiary terranes east of the Cascade Range (Tolan and Beeson, 1984; Evarts and O'Connor, 2008). In the southern part of the basin, Columbia River sediment interfingers with volcaniclastic debris transported by the ancestral Willamette River system. By the time local volcanism began in the late Pliocene, the topographic configuration of the Portland Basin was much like it is today.

CHARACTER AND SPATIAL DISTRIBUTION OF VOLCANIC CENTERS

Most mapped volcanic centers in the Boring Volcanic Field consist of variably degraded monogenetic cinder cones and spatially associated lava flows. Other vents are marked by small shields, domes, or exhumed subvolcanic intrusions. Olivine-phyric basalt and basaltic andesite dominate the field; andesites are rare but make up one of the larger edifices, the shield volcano at Larch Mountain (Fig. 3). Identification of vents that sourced the lava flows is generally unambiguous. Where possible, the association was confirmed with chemical analysis or petrographic

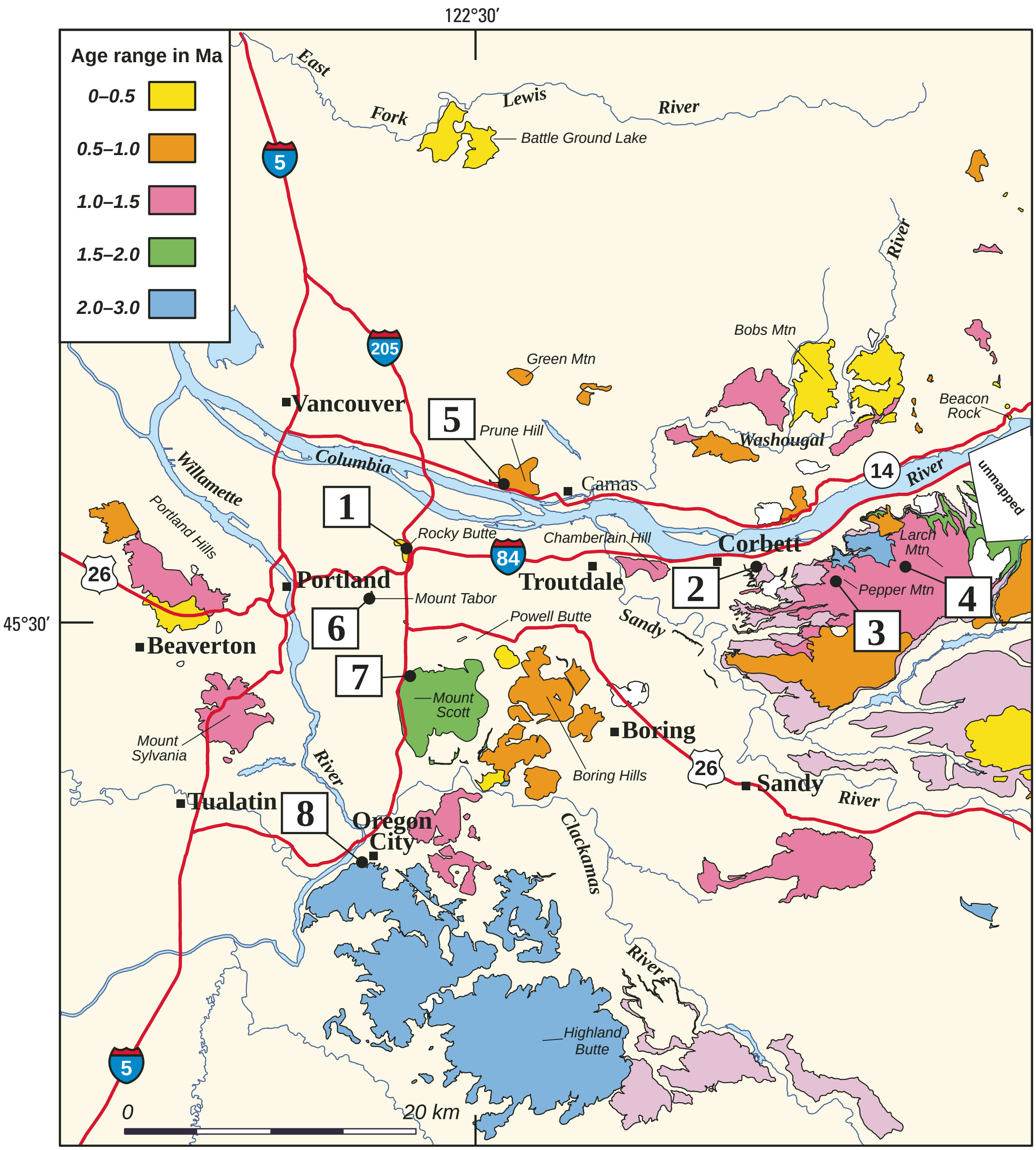

Figure 3. Map of the Boring Volcanic Field showing volcanic rocks grouped by age (Cascadian low-K tholeiite flows in mauve, undated units in white), geographic and cultural features referred to in text, and field trip stops.

comparison. In a few cases, source vents could not be located owing to erosion or burial and some units therefore consist only of morphologically or chemically distinctive lava flows. A small number of the vents on Figure 1 are only approximately located; a vent must exist, but its exact location within the area mapped as lava could not be determined. In some places, such as east of Oregon City and in the Bobs Mountain area (Fig. 3), chemically and petrographically similar flows apparently issued from several closely spaced vents, and it is not always possible to associate a flow with a specific vent. Phreatomagmatic deposits are less common than might be expected given the fluvial setting of the Portland Basin (White, 1991), presumably owing to rapid removal or burial in the large Columbia River system. The only morphologically intact maar is the young (≤100 ka) center at Battle Ground Lake (Fig. 3). All observed outcrops of volcanic breccia, however, contain rounded clasts of quartzite and other material incorporated from the Troutdale Formation, providing clear evidence of interaction with unconsolidated river deposits.

Using these criteria, we have identified nearly 80 individual centers in the Boring Volcanic Field. We believe that we have identified all exposed Boring centers within the Portland area (except for the incompletely mapped region on its eastern margin). Additional centers probably lie buried beneath younger sedimentary deposits, as suggested by aeromagnetic anomalies (Blakely et al., 1995) and water-well logs. The Portland Basin was severely impacted by the colossal latest Pleistocene (17,000–12,000 ^{14}C yr B.P.) Missoula Floods, which would have obliterated small cinder cones, tuff cones, and maars or buried them beneath as much as 30 m of slack-water silt (Waitt, 1994, 1996; Benito and O'Connor, 2003). Centers with extensive lava flows or vent-filling plugs, however, (Prune Hill, Rocky Butte, Beacon Rock; Fig. 3) survived the onslaught, so most likely only a few small vents remain undetected.

As is common in monogenetic volcanic fields (Connor and Conway, 2000), identified vents are not randomly dispersed but instead concentrated in clusters of 3–6 vents, commonly aligned, that erupted compositionally similar magma over short time spans. Examples include the Bobs Mountain and Portland Hills clusters (Fig. 3).

CHRONOLOGY OF BORING VOLCANIC ACTIVITY

Not all Boring centers provided suitable material for $^{40}Ar/^{39}Ar$ dating owing to weathering, fine grain size, or abundant glass. In addition, the systematics of many samples are complicated by excess Ar. We have obtained $^{40}Ar/^{39}Ar$ dates for ~80% of identified centers. We believe the available data are sufficiently comprehensive to provide a reasonably complete picture of the history of Boring Volcanic Field volcanism (Figs. 3 and 4).

In the eastern part of the Boring Volcanic Field south of the Columbia River, locally erupted volcanic rocks overlie lavas that apparently issued from vents near the axis of the Cascade volcanic arc to the east (Fig. 3; Conrey et al., 2004). These distally erupted lavas are coarse-grained, diktytaxitic, olivine ± plagioclase-phyric low-potassium tholeiites (LKT). Erupted between 3.3 and 3.0 Ma, these voluminous lavas and associated hyaloclastic sediments overwhelmed the ancestral Columbia River valley, eventually displacing the river to its present location where it carved the Columbia River Gorge (Tolan and Beeson, 1984). Preserved LKT sequences up to 200 m thick near the east edge of the Boring Volcanic Field consist of a multitude of thin flows. Interaction of these flows with the river generated large amounts of hyaloclastite, which was rapidly flushed downstream to be deposited in the Portland Basin (Tolan and Beeson, 1984; Evarts and O'Connor, 2008). The proportion of reworked-hyaloclastite interbeds in the LKT sequence increases westward and, at the east margin of the Portland Basin, the section consists largely of hyaloclastite-rich sediments with few lava flows. The hyaloclastite-rich deposits constitute the upper member of the Troutdale Formation of Tolan and Beeson (1984). Between latest Miocene and Pleistocene time, voluminous LKT lavas were emplaced in the northern Oregon Cascade Range, apparently related to intra-arc rifting (Conrey et al., 2004). The intensity of LKT volcanism along the arc axis in the Oregon decreased significantly after 3 Ma.

Local volcanism within the Boring Volcanic Field began in the southern part of the ancestral Portland Basin in latest Pliocene time. Between 2.6 Ma and 2.4 Ma, these eruptions produced (1) extensive basalt flows compositionally similar to the older Cascade-derived LKTs; (2) a large basaltic andesite shield volcano at Highland Butte; (3) several monogenetic basaltic andesite cinder cones and flows; and (4) an andesite flow. No documented volcanic activity occurred in the Portland Basin during the ensuing 750 k.y., although olivine-basalt flows were emplaced in the Cascade Range to the east at ca. 2.25 Ma (the vent for these flows has not been located but flow distribution suggests it lies buried beneath Larch Mountain volcano). LKTs continued to erupt in the arc to the east, and one large flow moved down the ancestral Clackamas River valley to enter the southern Portland Basin at 1.936 ± 0.010 Ma.

Volcanic activity in the Boring Volcanic Field resumed at ca. 1.6 Ma (Fig. 4) with the eruption of moderately alkalic basalts in

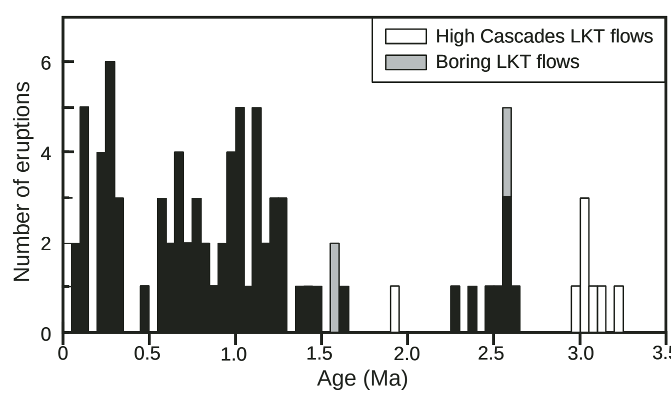

Figure 4. Frequency diagram showing age distribution of eruptions inferred from $^{40}Ar/^{39}Ar$ ages for Boring Volcanic Field (black and gray) and High Cascade low-K tholeiite (LKT) flows (white) in 0.05 m.y. bins.

the eastern part of the area and construction of the Mount Scott LKT shield volcano in the Portland Basin a few kilometers north of the late Pliocene centers. These were followed shortly thereafter by eruptions in the Cascade foothills, including those that built the Larch Mountain andesitic volcano. After ca. 1.3 Ma, volcanism became more widely distributed and compositionally diverse. By 1.0 Ma, volcanic centers had appeared in all parts of the Boring Volcanic Field. Activity has continued sporadically since that time, interrupted only by an apparent lull near 500 ka (Fig. 4). The youngest dated volcano in the Boring Volcanic Field is the massive plug of Beacon Rock at 57 ka, its enclosing cinder cone evidently having been stripped by the latest Pleistocene Missoula Floods. The undated maar at Battle Ground Lake, which was blasted through a ca. 100 ka lava flow, is the only other known vent likely to be much younger than ca. 100 ka.

Over the 2.6 m.y. history of the Boring Volcanic Field, there has been a poorly defined northward shift of volcanic loci in the Portland Basin. The southernmost part of the field experienced the oldest activity (ca. 2.6–2.4 Ma) and was last active at ca. 1.2 Ma. In contrast, all of the youngest (<300 ka) vents are located in the northern half of the field. The same trend is apparent in the Cascade foothills, where the vents in Oregon (except for two andesites that erupted from vents east of 122°W) were last active during the Matuyama Chron and younger vents are all north of the Columbia River.

PETROLOGY OF BORING LAVAS

Boring lavas are chiefly subalkaline basalts and basaltic andesites (Fig. 5A). They are geochemically diverse (Conrey et al., 2007), with a range nearly as large at that recorded in the entire southern Washington and northern Oregon Cascade arc segments (Leeman et al., 1990, 2005; Conrey et al., 1997; Bacon et al., 1997; Jicha et al., 2009). As illustrated by

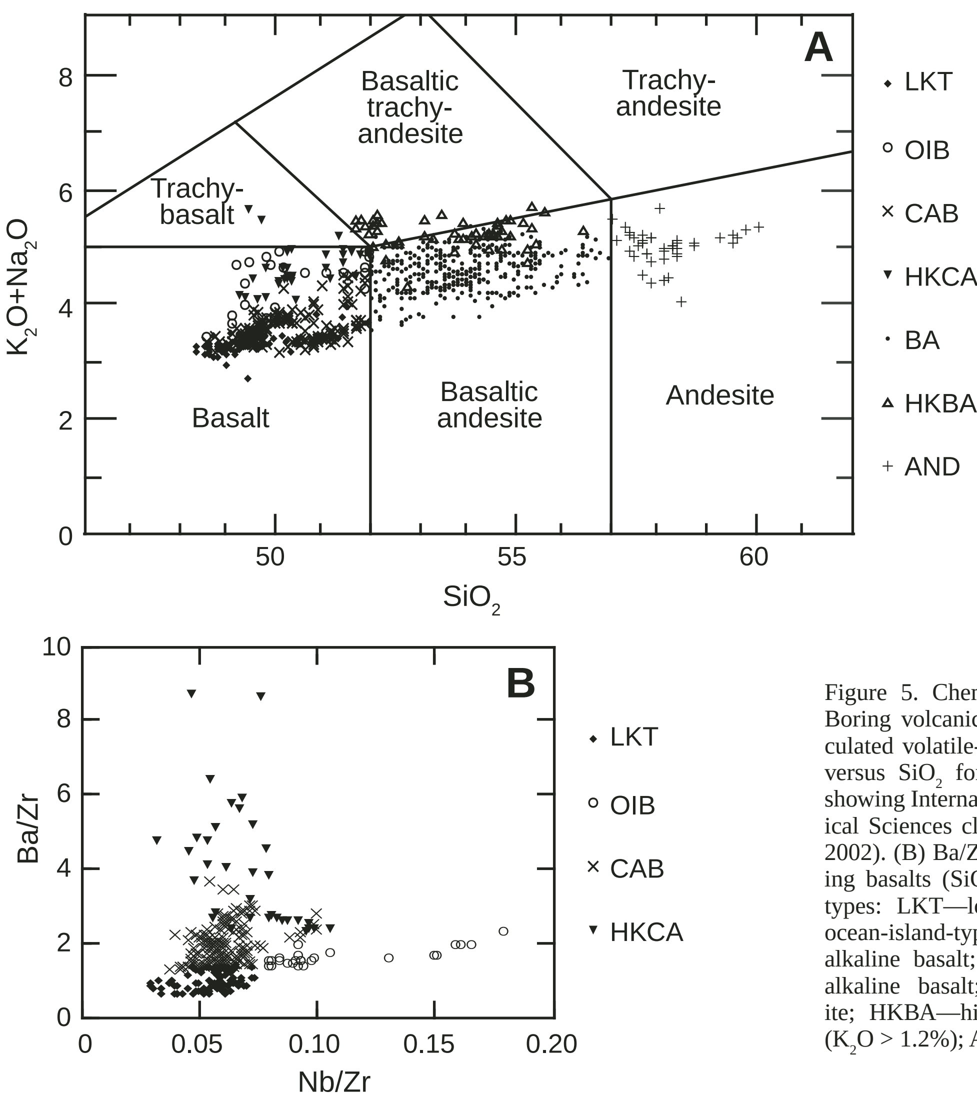

Figure 5. Chemical characteristics of Boring volcanic rocks (analyses recalculated volatile-free). (A) $K_2O + Na_2O$ versus SiO_2 for all Boring volcanics, showing International Union of Geological Sciences classification (Le Maitre, 2002). (B) Ba/Zr versus Nb/Zr for Boring basalts (SiO_2 < 52.0%). Chemical types: LKT—low-K tholeiite; OIB—ocean-island-type basalt; CAB—calc-alkaline basalt; HKCA—high-K calc-alkaline basalt; BA—basaltic andesite; HKBA—high-K basaltic andesite (K_2O > 1.2%); And—andesite.

basalt trace-element compositions (Fig. 5B), the Boring Volcanic Field includes magmas that appear related to subduction (Ba/Nb > 20) and those that do not. The subduction-influenced lavas (equivalent to Group II of Leeman et al., 2005) vary from abundant low- and medium-K calc-alkaline basalt (CAB) to minor high-K calc-alkaline basalt (HKCA; K_2O>1.3%), reflecting variable contributions of subduction-derived fluids to their mantle sources. Many Boring basalts, however, lack the relative enrichments in large-ion-lithophile elements that typify volcanic arc lavas. Instead, these lavas (equivalent to Group I of Leeman et al., 2005) range from low-K tholeiites that resemble mid-ocean ridge basalt (MORB) to ocean-island-like basalts (OIB) that are similar to magmas erupted at seamounts and other intraplate settings. The mineralogy of Boring volcanic rocks is consistent with the inferences derived from their chemical characteristics. Most LKTs and OIBs are aphyric, but porphyritic flows contain olivine and plagioclase phenocrysts, suggestive of dry magma, whereas CAB and HKCA basalts with more than 1% K_2O typically contain phenocrysts of olivine and clinopyroxene as well as groundmass phlogopite, consistent with wetter magmas (Conrey et al., 1997). However, even in the calc-alkaline lavas that do exhibit a subduction-zone signature, it is less pronounced than in lavas of most volcanic arcs (Leeman et al., 2004, 2005; Conrey et al., 2007). The relatively weak subduction signature, along with the abundance of MORB- and OIB-like basalts, suggest that the mantle wedge beneath southern Washington and northern Oregon is drier and warmer than those of most subduction systems. This inference is consistent with known parameters of the Cascadia subduction system, where the young (warm) Juan de Fuca plate is slowly converging with North America and, as a result, hydrous fluids are likely to be released from the downgoing slab at relatively shallow depths beneath the forearc (Van Keken et al., 2002; Hacker et al., 2003). Calculation of source temperatures and depths (Leeman et al., 2005) suggests that OIB come from the hottest, deepest part of the mantle wedge, whereas LKT are sourced at somewhat shallower depths. Both are interpreted as products of decompression melting of convecting asthenosphere. The geothermometric and geobarometric calculations also suggest that the CAB and HKCA come from a shallower, presumably lithospheric, source. This is consistent with areally restricted eruptions of compositionally similar basalts widely spaced in time (seen for example, in the Portland Hills and at Bobs Mountain), which imply the existence of long-lived, compositionally distinct, upper mantle or lower crustal domains.

Basaltic andesites form a large proportion of Boring centers (Fig. 5A) and are as chemically diverse as the basalts. No magnesian basaltic andesites like those in the southern part of the arc (Grove et al., 2005) have been found in the Boring field or the adjacent arc but some vents, such as Mount Tabor, produced primitive basaltic andesite potentially derived from CAB or HKCA. Other centers, such as Highland Butte, erupted lavas that appear to track the evolution of LKT during fractionation and crustal contamination. Basaltic andesite daughters of OIB parents have also been recognized. In general, the evolution from basalt to basaltic andesite of all chemical types is likely to have occurred in the deep crust, because most basaltic andesites are enriched in Al_2O_3 and Sr compared to basalt, and thus plagioclase was not a major crystallizing phase.

The scarce andesites found in the Boring Volcanic Field erupted from widely scattered monogenetic vents and the small Larch Mountain volcano. Most andesites are depleted in incompatible elements compared to associated basalts or to likely crustal source rocks, and may be fractionates of LKT (Smith et al., 2006). Rare Sr-rich and Y- and Nb-poor andesite, however, may be an independent magma, potentially generated by lower crustal melting at high temperature (Smith, 2008; Conrey et al., 2007).

The earliest Boring magmas were LKTs and related basaltic andesites that erupted in the southern part of the field. No LKTs appeared after 1.6 Ma, but otherwise we perceive no major volumetric or compositional trends within the Boring Volcanic Field. The vents of local clusters are commonly similar in age and geochemistry. For example, alkali-rich basalts erupted from several vents in the Bobs Mountain area at ca.120 ka, calc-alkaline basaltic andesites erupted from a cluster east of Oregon City at 1.20 Ma, and lavas with OIB-like compositions erupted from three or four centers north of Beacon Rock (Fig. 3) at ca. 1 Ma. In a few locations, eruption of compositionally similar lavas occurred at widely separated times; for example, hiatuses of ~1 m.y. separate eruptions of compositionally similar lavas in the Portland Hills and the Bobs Mountain clusters (Fig. 3).

SPECULATIONS ON THE TECTONIC SIGNIFICANCE OF BORING VOLCANISM

The presence of numerous basaltic vents in the forearc is confined to the southern Washington–northern Oregon section part of Cascadia and is certainly an unusual if not unique feature among subduction systems generally. The factors responsible for this tectonically anomalous volcanism are poorly understood but must reflect some atypical characteristics of the crust or upper mantle of this region. The most common explanation for forearc magmatism, subduction of a spreading center and formation of a slab window (e.g., Madsen et al., 2006), can't be invoked here.

The Boring Volcanic Field, which is the westernmost salient of a larger area of forearc magmatism in the southern Washington–northern Oregon arc segment (Hildreth, 2007), resembles most monogenetic volcanic fields in its low magmatic production rate, consistent with the absence of any heat-flow anomaly in the Portland area (Blackwell et al., 1990a, 1990b). Most Boring lavas are mafic and possess compositions indicating that they last equilibrated in the deep crust or mantle (Leeman et al., 2005). Eruption of small batches from such deep sources requires rapid passage through the crust in order to prevent freezing in transit. Some earlier accounts of Boring volcanism have inferred that vent locations occur along crustal faults (Allen, 1975; Blakely et al., 1995). Short vent alignments suggestive of fault control are apparent within some local clusters but evidence for strong control by major structures is lacking (Figs. 1 and 3). This is consistent with the near-absence of large, through-going crustal faults in the Portland Basin and with the diffuse seismicity that characterizes the region (Yelin and Patton, 1991; Blakely et al., 1995, 2000). NW-striking dextral strike-slip and oblique-slip faults have been mapped along the SW margin of the Portland Basin but vents are no more abundant or more strongly aligned there than elsewhere in the field. The ephemeral conduits for the low-volume Boring eruptions may be localized at short-lived releasing bends along distributed structures that form and rapidly close in a continuously changing local stress field.

Boring LKTs are similar to Pliocene rift-related basalts erupted along the axis of the Cascade volcanic arc to the east, and the crude northward shift of volcanic loci in the Boring Volcanic Field mimics the pattern of volcanism related to northward-propagating rifting of the arc (Conrey et al., 2004). Boring volcanism began shortly after LKT volcanism largely ended in the Mount Hood area, and the Boring Volcanic Field can be viewed as a northwestward extension and continuation of this rift-related volcanism. Rifting of the arc axis and volcanism in the forearc may both be ultimately related to the clockwise rotation and northward transport of the Oregon Coast Range microplate owing to oblique subduction (Wells et al., 1998; McCaffrey et al., 2007). One implication of this model is that the Boring Volcanic Field is localized in space and time by crustal dynamics rather than by the thermal regime of the forearc mantle. That is, partial melt may be present in the mantle beneath much of the Cascadia forearc, but only in the Portland area, at the north end of the rigid, rotating Oregon Coast Range block, has fracturing of the crust created a plumbing system that permits its extraction.

Alternatively, or additionally, there may be something peculiar about the mantle wedge in this part of Cascadia. Because the Oregon continental margin is virtually aseismic, the configuration of the subducting Juan de Fuca plate is poorly known. Recent seismic models infer that the top of the plate is only 50 km beneath Portland, but the limited data on which the models are based require simplifying assumptions and are insufficient to resolve local complexities (Flück et al., 1997; McCrory et al., 2005). Such a shallow slab is difficult to reconcile with mafic volcanism, particularly if the wedge tip is serpentinized and therefore cold (Bostock et al., 2002; Blakely, et al., 2005) and implies the existence of strong lateral and vertical temperature gradients in the mantle beneath the forearc (Leeman et al., 2005). A tear or other discontinuity in the Juan de Fuca plate (Michaelson and Weaver, 1986; Wilson, 1988, 2002) that would allow hot asthenosphere from the subarc or beneath the slab to convect into the wedge corner would seem to be required. Furthermore, any model to fully explain the anomalous tectonic position of Boring volcanism must also account for its recency, yet there is scant evidence for a significant change in the convergence parameters in Cascadia in the past 10 Ma (Wilson, 2002).

VOLCANIC-HAZARDS IMPLICATIONS

All Boring volcanic centers are extinct, but the Boring Volcanic Field presumably is not. The most recent eruptions in Portland-Vancouver metropolitan area occurred ~100,000 years ago and the age of youngest dated center, Beacon Rock at the east edge of the Boring Volcanic Field, is 57 ka. Rarely has 50,000 years passed without an eruption (Fig. 4). If we treat each mapped vent as representing a distinct eruption, and assume that mapped but undated centers (~20% of the total) would exhibit the same frequency pattern as the dated ones, and that the number of undetected eruptions is no greater than 10% of the total, we estimate an average of roughly 1 eruption every 15,000 years since the main period of volcanism began ca. 1.6 Ma. We recognize the difficulties inherent in simply equating vents with eruptive events (Connor and Conway, 2000) but suspect that any overcounting resulting from multi-vent eruptions is largely balanced by counting the larger polygenetic edifices as single eruptions.

Approximately half of these eruptions took place in what are now densely populated portions of the Portland-Vancouver metropolitan area. The probability of an eruption in the metro area is thus very low, considerably less than that of an eruption in the High Cascade Range or a major earthquake on the Cascadia megathrust (every 500 years). Furthermore, unlike earthquakes, formation of a typical Boring volcano would affect a relatively small area. Nevertheless, depending on location, the consequences could extend well beyond the few km^2 that would be buried by a cinder cone and lava flows. Ash would blanket areas downwind of the vent and major infrastructure elements could sustain considerable damage. Eruptions of individual monogenetic centers typically last only a few days to a few months (Wood, 1980) but larger outpourings such as those that built Mount Sylvania and Larch Mountain may have extended for years to decades. The widespread spatial and temporal distribution of Boring vents makes it difficult to predict where eruptions are most likely, but all eruptions in the past 300,000 years have occurred in the northern part of the Boring Volcanic Field.

ROAD LOG

On this one-day trip we will visit seven sites that provide representative samples of Boring volcanic centers exhibiting varying eruptive styles, ages, and petrology. Chemical analyses, paleomagnetic vectors, and $^{40}Ar/^{39}Ar$ ages for these units are given in Tables 1 and 2. $^{40}Ar/^{39}Ar$ analytical data for incremental-heating experiments are provided in Table 2 and paleomagnetic data are provided in Table 3 and shown in Figure 6. Road log begins at Oregon Convention Center. Datum for geographic coordinates is NAD27.

Mileage	*Description*
0.0	Leave convention center heading south on NE Martin Luther King Jr. Blvd.

TABLE 1. CHEMICAL ANALYSES, RADIOMETRIC AGE DATES, AND PALEOMAGNETIC ORIENTATIONS FOR VOLCANIC UNITS VISITED ON FIELD TRIP

	1	2	3	4	5	6	7	8	9
Sample no.:	QV99-18	03BV-G174	BVCK-1	03BV-G135	03BV-G128s	99CM-T03	QV99-21B	RC02-143	RC02-11B
Center/Unit:	Rocky Butte	LKT	LKT	Brower Road	Larch Mountain	Prune Hill	Mount Tabor	Mount Scott	Canemah
Latitude (°N):	45°32.387'	45°32.000'	45°32.174'	45°31.404'	45°32.253'	45°35.154'	45°30.940'	45°28.142'	45°20.942'
Longitude (°W):	122°33.724'	122°14.878'	122°10.093'	122°10.908'	122°06.845'	122°28.669'	122°35.753'	122°33.517'	122°36.518'
Age (ka):	285 ± 16	—	3110 ± 90	1260 ± 10	1430 ± 50†	590 ± 50†	203 ± 5	1552 ± 14‡	2572 ± 13‡
Magnetic Polarity:	N	N	N	R	R	N	—	R	R
Inclination:	59.1	53.6	54.5	–60.8	–49.3	49.2	—	–43.2	–51.5
Declination:	1.8	359.8	10.9	201.7	181.7	22.8	—	165.9	192.1
α_{95}:	1.3	3.2	7.2	5.7	3.8	4.3	—	3.2	2.1
Major elements (wt%)									
SiO_2	54.41	49.62	48.84	49.62	57.83	54.39	53.78	50.30	51.40
TiO_2	1.24	1.30	1.35	1.40	1.00	1.26	1.17	1.40	1.24
Al_2O_3	17.26	17.23	17.36	15.57	17.75	17.25	17.02	17.44	16.66
FeO*	7.25	11.81	11.63	8.48	6.47	7.83	7.38	10.21	10.01
MnO	0.12	0.18	0.19	0.13	0.11	0.13	0.12	0.19	0.16
MgO	6.28	7.31	7.34	8.31	4.19	6.06	6.76	7.23	7.76
CaO	7.85	9.01	10.04	10.35	7.26	7.82	8.21	9.50	9.21
Na_2O	4.08	3.10	3.01	3.71	4.08	3.86	3.89	3.10	3.01
K_2O	1.17	0.31	0.13	1.71	1.10	1.07	1.27	0.42	0.38
P_2O_5	0.35	0.13	0.12	0.71	0.22	0.34	0.39	0.20	0.17
Original total	99.50	99.40	97.51	98.24	100.67	99.83	99.00	98.90	100.22
Mg#	64.5	56.5	57.0	67.3	57.6	61.9	65.7	56.1	62.0
Trace elements (ppm)									
Ba	341	120	59	1324	312	426	586	194	135
Rb	18	3	1	9	18	11	10	3	3
Sr	828	301	228	2907	594	780	1089	410	396
Y	18	22	24	14	19	21	19	28	21
Zr	167	70	82	152	147	151	155	94	96
Nb	8.7	3.4	4.1	7.1	7.9	10.8	8.9	6.1	6.2
Ni	129	135	115	174	55	125	164	139	115
Cu	52	56	63	71	55	55	56	74	45
Zn	80	91	89	106	76	93	78	84	86
Cr	178	197	236	265	60	197	225	210	201
Sc	19	29	31	22	18	19	21	31	32
V	161	194	195	193	139	151	158	197	177

Note: X-ray fluorescence analyses performed at GeoAnalytical Laboratory of Washington State University using methods described in Johnson et al. (1999). Major element analyses recalculated anhydrous and normalized to 100%. FeO*, total Fe calculated as FeO; Mg#, atomic ratio 100Mg/(Mg+Fe^{2+}) with Fe^{2+} set to 0.85x Fe^{total}. —, not determined. See Tables 2 and 3 for details of $^{40}Ar/^{39}Ar$ and paleomagnetic measurements. LKT—low-K tholeiite.

†K-Ar age from Conrey et al. (1996a).

‡Age determination from different locality within same unit.

TABLE 2: $^{40}Ar/^{39}Ar$ DATA FOR BORING UNITS AND CASCADIAN LOW-K THOLEIITE FLOWS VISITED ON FIELD TRIP

Sample no.	Unit	[1]Material	[2]Total-gas age (Ma)		[3]Plateau age (Ma)			[4]Isochron age (Ma)				[5]Age at Cl/K min		[6]Indicated age (Ma)		Comment
			Age	±1σ	Age	±1σ	[7]MSWD	Age	±1σ	MSWD	Intercept (±2σ)	Age	±1σ	Age	±1σ	
03BV-G135	Brower Road	GM	1.23	0.01	1.260	0.010	1.8	1.276	0.051	22	293.5 ± 8.2	1.25	0.02	1.26	0.01	
99CM-T03	Prune Hill	WR	0.933	0.012	0.730	0.011	0.40	0.7	0.17	37	309 ± 24	*none*		<0.73	0.011	Excess Ar; maximum age
BVCK-1	Cascade LKT	GM	3.107	0.071	3.015	0.073	1	3.15	0.25	0.73	293.6 ± 4.3	3.01	0.11	3.015	0.073	
QV99-18	Rocky Butte	WR	0.285	0.016		*none*		0.310	0.046	276	294.8 ± 5.0	*none*		0.285	0.016	Complex recoil/ excess Ar
QV99-21B	Mount Tabor	GM	0.195	0.016	0.203	0.005	1.4	0.212	0.015	1.9	294.1 ± 4.9	0.211	0.009	0.203	0.005	
RC02-154	Mount Scott	GM	1.490	0.017	1.552	0.014	1.8	1.54	0.060	4.2	295.5	1.55	0.06	1.552	0.014	Isochron forced
RC93-17	Mount Scott	GM	1.540	0.667	1.599	0.042	0.67	1.626	0.059	0.38	294.3 ± 3.0	1.625	0.047	1.599	0.042	
RC02-190	Canemah	GM	2.578	0.011	2.572	0.013	1.6	2.57	0.06	1.9	296.1 ± 9.4	2.566	0.047	2.572	0.013	

[1]GM is groundmass of the basaltic samples, and WR is whole rock.
[2]Total-Gas age is the age calculated from the sum of all radiogenic ^{40}Ar divided by the sum of all potassium-derived ^{39}Ar in an age-spectrum (incremental-heating) experiment.
[3]An $^{40}Ar/^{39}Ar$ plateau age is the weighted mean age of contiguous steps representing at least 50% of the potassium-derived ^{39}Ar released in an incremental-heating experiment and for which ages are concordant at the 95% level of confidence (Fleck et al., 1977).
[4]The isochron age is calculated by weighted-error regression of the $^{40}Ar/^{36}Ar$ and $^{39}Ar/^{36}Ar$ of contiguous gas fractions representing at least 50% of the potassium-derived ^{39}Ar released in an incremental-heating experiment. Ar isotopic ratios are corrected for reactor-derived interfering isotopes.
[5]The weighted mean age of the step or steps of an incremental-heating experiment that define a minimum in a systematic variation of the Cl/K ratio.
[6]Indicated age represents the age calculated by the reduction technique considered the most reliable of the four reported on the basis of interpretation of the $^{40}Ar/^{39}Ar$ age spectrum.
[7]MSWD represents mean-square of weighted deviates, a measure of goodness of fit, comparing the observed scatter to that expected from calculated analytical errors (McIntyre et al., 1966).

TABLE 3. PALEOMAGNETIC DATA FOR BORING UNITS AND CASCADIAN LKT FLOWS VISITED ON FIELD TRIP

Lab no.	Field no.	Unit	λ_S	ϕ_S	I	D	N/N_0	R	k	α_{95}	λ_P	ϕ_P
T0260	QV99-18	Rocky Butte	45.538	122.564	59.1	1.8	7/8	6.9971	2047	1.3	84.2	43.8
4T184	03BV-G174	Cascadian LKT	45.533	122.248	53.6	359.8	8/8	7.9767	300	3.2	81.3	58.7
4T175	BVCK-1	Cascadian LKT	45.545	122.168	54.5	10.9	5/9	4.9648	114	7.2	76.6	15.9
T0268	99CM-T03	Prune Hill	45.587	122.486	49.2	22.8	7/8	6.9699	199	4.3	66.4	0.6
4T152	03BV-G135	Brower Road	45.523	122.182	–60.8	201.7	6/7	5.9637	138	5.7	73.9	333.4
4T159	03BV-G128s	Larch Mountain	45.537	122.115	–49.3	181.7	7/8	6.9759	249	3.8	74.5	52.4
4T248	RC02-143	Mount Scott	45.470	122.558	–43.2	165.9	7/8	6.9830	353	3.2	66.8	91.5
T2239	RC02-11B	Canemah	45.349	122.609	–51.5	192.1	8/8	7.9899	693	2.1	73.8	162.0

Note: λ_S and ϕ_S are north latitude and west longitude of site in degrees, I and D are in situ inclination and declination of mean paleomagnetic directions in degrees, N/N_0, number of samples averaged/number of samples collected, R, vector sum of N unit vectors, k is concentration parameter (*Fisher*, 1953), α_{95} is radius of 95% confidence in degrees, λ_P and ϕ_P are north latitude and west longitude of corrected virtual geomagnetic pole in degrees. LKT—low-K tholeiite.

0.2 At south end of I-84 overpass, turn left onto Everett St. In one block, at Grand Avenue, bear slightly left onto I-84 eastbound ramp.
4.7 Take exit 5. At end of ramp, turn right onto Multnomah Street.
5.0 Turn right onto 82nd Avenue (OR 213).
6.1 Turn right at light onto Fremont Street (Portland Bible College).
6.5 Road swings to left, becoming 91st Street.
6.8 Road bends east, becoming Rocky Butte Road, and runs along top of north-facing cliff formed by a columnar-jointed sill or valley-filling flow >400 ft (120 m) thick.
7.5 Basaltic andesite crops out from retaining wall on right.
7.8 Joseph Wood Hill Park at summit of Rocky Butte, park on right side of road and climb steps to viewing area.

Stop 1: Joseph Wood Hill Park on Rocky Butte (45.54677°N, 122.56469°W)

Rocky Butte, a prominent isolated hill within the Portland city limits (Figs. 3 and 7), is the eroded intrusive core of a late Pleistocene basaltic andesite center. The park at the summit (elevation ~600 ft [200 m]) was constructed by the Works Progress Administration in the 1930s. Rock extracted from quarries on the east side of the butte was used to construct the Multnomah County jail, which was demolished in the 1980s during construction of I-205 below. The rock from the jail was then recycled to renovate parts of the Historic Columbia River Highway, on which we will travel later in the day.

The view from the observation deck encompasses most of the Boring volcanic field as well as Mount St. Helens to the north and Mount Hood to the east. The low forested hills to the southeast are the Boring Hills, from which the name of the volcanic field is derived. Many of the isolated low hills scattered through the urban area are volcanic centers or consist of fluvial gravels that have volcanic rocks on them. They include, clockwise from the north, Green Mountain, Prune Hill (Fisher Quarry), Chamberlain Hill, Devils Rest, Larch Mountain (with its pronounced prow), Pepper Mountain, Powell Butte (in front of the Boring Hills), Kelly Butte, and Mount Tabor. To the west, downtown Portland sits at the base of the Portland Hills, a northwest-striking anticlinal ridge capped by a few small Boring centers. Directly east is the mouth of the Columbia River Gorge. About 17,000 years ago, the colossal glacier-outburst Missoula Floods poured out of the gorge taking dead aim at the Rocky Butte volcano, stripping away the cinders that likely enclosed the massive basaltic andesite we stand on and producing a pronounced arcuate moat-like depression on the butte's east side.

The summit park is probably within the throat of the vent judging from the abundant oxidized scoriaceous rock in nearby

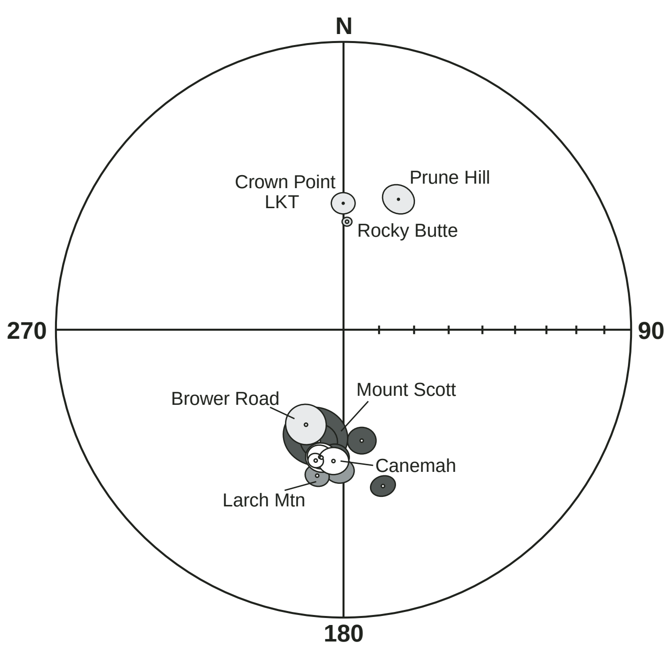

Figure 6. Paleomagnetic orientations determined for Boring units visited on trip; data from Table 3. LKT—low-K tholeiite.

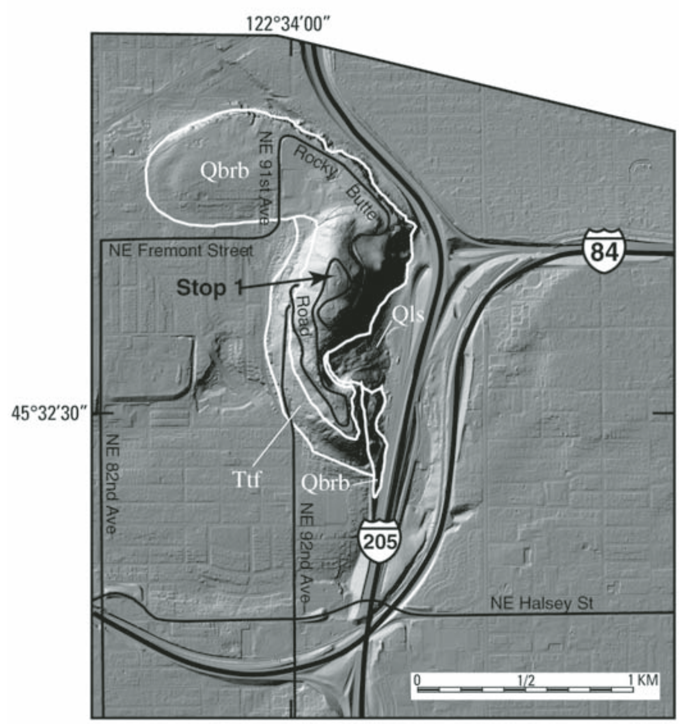

Figure 7. Geology of Rocky Butte (Stop 1) on hillshade image derived from LiDAR digital elevation model. Qbrb—basaltic andesite of Rocky Butte; Ttf—Troutdale Formation; Qls—landslide deposit.

roadcuts. Only basaltic andesite is exposed from the park down to the interstate but to the south, a debris flow scarp on the east slope of the butte reveals fluvial gravel of the Miocene–Pliocene Troutdale Formation intruded by a basaltic andesite sill, and Allen (1957) reported a dike cutting deformed Troutdale gravel in an abandoned quarry on the west side of the butte.

Rocky Butte consists of olivine-phyric, calc-alkaline basaltic andesite (Table 1, #1), a composition typical of many Boring centers. An $^{40}Ar/^{39}Ar$ experiment on a sample from a roadcut on I-205 at the south end of butte (Table 2) exhibited complex recoil effects and excess Ar; it did not yield a plateau. Its total gas age of 285 ± 16 ka (Table 2) is the best estimate of its age, which is consistent with its normal magnetic polarity (Fig. 6).

Mileage	*Description*
7.8	Leave Joseph Wood Hill Park, turning right at end of parking area onto Rocky Butte Road.
8.3	Communications tower at south end of Rocky Butte.
8.5	Exposures of near-vent agglomerate in roadcuts on right for next 0.3 mi.
8.8	Tunnel.
9.0	Stonework retaining wall holds back poorly consolidated gravel.
9.2	Stop sign; continue straight on 92nd Avenue.
9.7	Left onto Halsey Street.
11.2	Left onto 122nd Avenue.
12.0	Turn right onto I-84 eastbound to Troutdale–Hood River.
18.2	Outcrop on left of massive hyaloclastic sandstone of Troutdale Formation.
19.4	Sandy River. Slope along south side of highway for next several miles is Troutdale Formation capped by early Pleistocene lava flows erupted from Chamberlain Hill. Prominent notch on skyline directly ahead is at summit of Larch Mountain volcano.
23.6	Take Exit 22 (Corbett), turn right at stop sign onto Corbett Hill Road. Quarry directly to right and roadcuts ahead are in Columbia River Basalt.
24.8	Road climbs up through Troutdale Formation gravels. Bench formed on top of subhorizontal Columbia River Basalt flows.
25.2	Take left fork to stop sign; turn left onto Historic Columbia River Highway.
25.4	Corbett Market.
26.7	Portland Women's Forum State Scenic Viewpoint. Highway runs along headscarp of Rooster Rock landslide.
27.0	Just before junction with Larch Mountain Road, pull off and park on left side of highway. Walk eastward on highway ~0.3 mi to next stop. Watch for traffic.

Stop 2: Crown Point lava flow (45.53271°N, 122.24863°W)

The highway cuts across the upper part of the Rooster Rock landslide scarp, offering 0.5 mi of continuous roadcut exposure of the Troutdale Formation and an interbedded lava flow (Figs. 3 and 8). The columnar-jointed flow is a late Pliocene low-potassium tholeiite (LKT) that probably issued from a fissure vent in the Cascade Range near Hood River. We interpret it as one of the most far-traveled of many flows that erupted near the axis of the Cascade arc in late Pliocene time (Conrey et al., 1996b, 2004) and moved westward down a broad Columbia River paleovalley toward the ancestral Portland Basin. The appearance of this flow is typical of LKT: coarse grained, olivine- and plagioclase-bearing, and diktytaxitic. Chemically, it (Table 1, #2) is somewhat richer in K, Rb, Sr, and Ba than most LKT (compare Table 1, #3). No $^{40}Ar/^{39}Ar$ age has been determined for this flow but a LKT flow interbedded with Troutdale Formation sediments in Bridal Veil Creek, ~6 km east of here, gave an age of 3.015 ± 73 Ma (Table 2). Both of these flows have normal paleomagnetic polarities, indicating emplacement during the Gauss Chron. Other, stratigraphically lower, LKT flows that we have sampled have reversed magnetic polarities and were presumably emplaced during the Kaena or Mammoth Subchrons. The oldest age we have obtained for Cascadian LKT flows is 3.5 Ma for a flow near the base of the LKT section at Hood River, Oregon.

The fluvial deposits above and below the flow contain palagonitized sideromelane (basaltic glass) as a major component. Fresh sideromelane from several localities in the Portland area has a composition like that of the interbedded LKT flows (Swanson, 1986). Large quantities of hyaloclastite were evidently formed when voluminous LKT flows entered the ancestral Columbia River to the east (Waters, 1973). Although previous workers have

Figure 8. Low-K tholeiite flow overlying Troutdale Formation on Historic Columbia River Highway south of Crown Point (Stop 2).

referred to these Pliocene LKT flows as Boring lavas, we exclude them because they were not erupted from local vents.

Continue east on Historic Highway to Vista House at Crown Point. The Troutdale Formation is well exposed in road cuts. The coarse-grained and poorly sorted sediments exhibit steep foreset bedding and other features indicative of rapid transport and deposition in major floods.

Vista House, constructed shortly after the Historic Columbia River Highway was opened in 1915, sits atop a ~225-m-thick intracanyon flow of the Columbia River Basalt Group. Columbia River Basalt flows form most of the cliffy terrain of the western Columbia River Gorge. These huge flood-basalt flows, some larger than 3000 km^3, issued from fissures in what is now western Idaho and eastern Oregon and Washington in Miocene time to form the world's youngest flood-basalt province (Tolan et al., 1989). Many of the largest flows transected the ancestral Cascade Range through a 50-km-wide paleo–Columbia River valley and some of them eventually reached the Pacific Ocean (Wells et al., this volume). The Columbia River Gorge is a relatively recent feature (Tolan and Beeson, 1984) incised near the northern edge of the trans-arc paleovalley.

Several volcanoes of the eastern part of the Boring Volcanic Field can be seen from here including Mount Pleasant and Mount Zion, with Bobs Mountain in the background, across the Columbia River in Washington. Upriver to the east is Beacon Rock, a basaltic andesite neck that is the youngest dated Boring center, at 57 ka. Boring centers that are also visible south of the river in Oregon include Devils Rest, Pepper Mountain, and Larch Mountain.

Reset odometer to 0.0.

Mileage	*Description*
0.5	Turn sharply to left onto Larch Mountain Road.
2.0	Haines Road; stay to right. Road here runs along northeast flank of Ross Mountain, a high-silica basaltic andesite center largely buried by Pleistocene loess. Rare outcrops are deeply weathered and we found no material suitable for dating.
3.1	View of Larch Mountain and Pepper Mountain at 10 o'clock.
3.8	Junction with Louden Road; bear left. Louden Road runs on the surface of a lava flow toward its source at Pepper Mountain.
4.6	Junction with Brower Road; turn left.
5.6	Pull into rockpit on right.

Stop 3: Brower Road rockpit (45.52339°N, 122.18203°W)

The platy basalt in this small rockpit (Fig. 3) erupted from a vent ~1.5 km southeast of here. The hill above, Pepper Mountain, is a younger, compositionally different cinder cone. The flow in the pit is an absarokite (trachybasalt), the most highly large-ion lithophile–enriched (Ba/Nb = 187) composition in the Boring Volcanic Field (Table 1, #4; Conrey et al., 1997). Its high-K composition is manifested in the presence of abundant phlogopite in the groundmass and vesicles. It is unique in the Boring Volcanic Field in containing augite phenocrysts with cores of cloudy aluminous augite of likely crustal origin (A. Jones and M. Streck, unpublished data). This flow is magnetically reversed (Fig. 6) and yielded an $^{40}Ar/^{39}Ar$ plateau age of 1.26 ± 0.01 Ma (Table 2). Turn around and return to Larch Mountain Road.

Mileage	*Description*
6.7	Turn left onto Larch Mountain Road.
11.6	Pull off to left of road.

Stop 4: Andesite of Larch Mountain (45.53753°N, 122.11405°W)

Larch Mountain is a small shield volcano and one of the larger centers in the Boring Volcanic Field (Fig. 3). Its flows are petrographically distinctive, containing phenocrysts and glomerocrysts of coarse olivine ± augite in a plagioclase-microphyric groundmass. Chemically the flows are relatively uniform low-silica andesites (Table 1, #5). Conrey et al. (1996a) obtained a conventional K-Ar age of 1.43 ± 0.05 Ma from this outcrop. Larch Mountains flows are magnetically reversed (Fig. 6).

The road continues for another 5 mi to Sherrard Point at the summit of Larch Mountain. Five Cascade stratovolcanoes (Rainier, St. Helens, Adams, Hood, and Jefferson) can be seen from that viewpoint, which sits atop a cirque carved into an andesite plug that fills the vent of Larch Mountain volcano. Because of time constraints, we will not continue further but instead retrace our route back to Portland.

Mileage	*Description*
16.4	Brower Road.
17.2	Louden Road.
20.5	Junction with Historic Highway.
22.4	Right onto Corbett Hill Road to I-84.
23.8	Enter I-84 westbound. ***Reset odometer to 0.0.***
11.5	Best to be in center lane; follow signs to I-205 northbound/Seattle; Rocky Butte directly ahead.
12.6	Bear left at split.
13.0	Take right exit onto I-205 northbound.
15.2	Glenn L. Jackson Bridge over Columbia River.
15.9	Government Island.
17.4	Take Exit 27 to WA 14; take left exit lane (Camas).
21.8	Take Exit 10, 192nd Ave; turn left at top of ramp; stay in right lane.
22.6	Right turn onto Brady Road.
22.7	Pull off on right.

Stop 5: Fisher Quarry
(45.58610°N, 122.47035°W)

The large Fisher Quarry has been in more or less continuous operation for over a hundred years (Darton, 1909). Excavated rock is used chiefly for road base and landscaping purposes; large blocks (>30 tons) have been used to construct jetties at the mouth of the Columbia River.

The quarry is developed in a set of flows or flow lobes that erupted from a vent located on the slope of Prune Hill to the east (Fig. 3). Beds of agglutinated scoria and a clastogenic lava flow crop out on the steep forested south slope of Prune Hill. The lava flows exhibit well developed columnar jointing and scoriaceous flowtop breccia. At the stop, lava rests on west-dipping scoria beds that were nicely exposed during construction of the freeway interchange in 2002 (Fig. 9).

The flows consist of olivine-phyric basaltic andesite (Table 1, #6), rather similar to the Rocky Butte flows. The rock contains substantial interstitial glass, rendering it problematic for geochronology. Conrey et al. (1996a) report a K-Ar whole-rock age of 590 ± 50 ka for a sample from a roadcut on SR 14. Our attempt to obtain an $^{40}Ar/^{39}Ar$ date for a sample collected south of the highway, where lava rests on river gravels, yielded a maximum age of 730 ka (Table 2). The lava is normally polarized (Fig. 6).

Reset odometer to 0.0.

Mileage	*Description*
0.0	Return to 192nd Avenue; turn left.
0.3	Turn right onto SR 14 westbound.
3.7	Bear right onto exit road to I-205.
4.3	Right exit onto I-205 southbound.
9.9	Take Exit 21A; follow signs to Stark Street.
11.0	Turn right onto (one-way) Stark Street. Mount Tabor directly ahead.
12.0	At base of Mount Tabor, road turns to right, becomes Thorburn Street. Best to be in left lane.
12.2	Three-way split at light. Take middle road (slightly to left and uphill) to remain on Thorburn Street, which shortly becomes Stark Street again.
12.9	Left at light onto 60th Avenue.
13.1	Left at light onto Belmont Street, climbing up Mount Tabor.
13.5	Right at stop sign onto 69th Avenue.
13.7	Enter Mount Tabor Park. Turn right on Salmon Way to volcano.
13.9	Parking lot on right.

Figure 9. Basaltic andesite of Prune Hill flow overlying black to oxidized scoria beds near Fisher Quarry (Stop 5). Outcrop is ~12 m high.

Stop 6: Mount Tabor Park
(45.51570°N, 122.59586°W)

Mount Tabor, although commonly referred to as an extinct volcano, consists mostly of Troutdale Formation gravels, but the remnant of a small cinder cone is beautifully exposed behind the outdoor amphitheater on its northwest flank (Figs. 3 and 10). The volcanic character of this feature was recognized shortly after the park was established in 1909 and the eastern half of the cone was removed early on to provide material for paths, roads, and walls in the park. Fortunately for us, efforts by the Geological Society of the Oregon Country saved the cone from complete obliteration.

The cinder-cone cross-section is small yet complicated, revealing some of the complexities of cone formation during a pulsing eruption. Note the local unconformities, faults, abrupt dip reversals, and the variations in grain size, sorting, and agglutination. A small, chemically similar, lava flow issued from the base of the cone and flowed to the north; it is no longer exposed owing to residential development. A pronounced positive aeromagnetic anomaly is associated with Mount Tabor (Snyder et al., 1993; Blakely et al., 1995), suggesting that it is cored by a subvolcanic intrusion. Compositionally, the cinders and lava flow are relatively primitive, alkali-rich basalt (Table 1, #7). The black scoria below the oxidized weathered horizon is remarkably fresh, suggesting relative youth. An $^{40}Ar/^{39}Ar$ plateau age 203 ± 5 ka was obtained from this outcrop (Table 2). Return to bus and retrace route to I-205.

Mileage	*Description*
14.1	Turn left onto 69th Avenue.
14.2	Left onto Belmont Street.
14.7	Right onto 60th Avenue.
14.9	Right onto Stark Street.
15.8	Road curves into Washington Street (one-way).
16.0	Cross 82nd Avenue (SR 213). Move into right lane.
16.8	Right onto I-205 southbound. Directly ahead is Kelly Butte with Mount Scott behind it.

17.9	Freeway rises on west flank of Kelly Butte.
18.1	Quarry behind church to east of freeway exposes basaltic andesite flow resting on fluvial sediments and vent breccia and overlain by gravel. Flow is ca. 1 Ma, erupted during the normal-polarity Jaramillo subchron. Same flow was exposed during construction of light-rail line along west side of freeway. Mount Scott at 11 o'clock.
19.1	Exit 17 to Foster Road. Get into right lane.
19.2	Turn right onto Foster Road. Move to left lane.
19.3	Left onto 92nd Avenue. Stay in right lane to remain on 92nd.
20.0	Left at light onto Flavel Street.
20.2	Left onto Knapp Street just before Flavel climbs up slope of Mount Scott.
20.5	Pull over on side of road; abandoned rockpit on right.

Stop 7: Knapp Street Quarry, basalt of Mount Scott (45.46946°N, 122.55906°W)

Massive basalt crops out at the top of the slope above the road. Exposures in the walls of the small creek reveal beds of palagonitic hyaloclastite and underlying gravels. Mount Scott (Fig. 3) is a shield volcano, one of the larger centers in the Boring field. The flows exhibit LKT compositions similar to the Cascadian LKT flows (Table 1, #8) but were erupted locally. The palagonitic sandstones and gravels indicate basalt-water interaction in a fluvial setting. Generation of hyaloclastite was likely a common occurrence during eruptions within the ancestral Portland Basin, but deposits of these events are rarely preserved except where, as here, they were buried and protected by lava flows. All Mount Scott lavas sampled exhibit reversed polarities (Fig. 6). Ages obtained for Mount Scott lavas are 1.6–1.5 Ma (Table 2). These eruptions ended a roughly 750,000 yr quiescent period and began a period of relatively continuous activity that continued into the late Pleistocene (thus far). This was the last time that LKTs erupted in the Boring Volcanic Field. Turn around to return to I-205.

Mileage	*Description*
20.8	Right onto Knapp Street.
21.0	Right onto 92nd Avenue.
21.3	Right onto Foster Road.
21.4	Right onto I-205 southbound ramp.
24.1	Basalt of Mount Scott in roadcut, east side of freeway.
24.7	Mount Talbert at 9 o'clock. Another Boring basaltic andesite center, dated at 857 ± 6 ka.
28.3	Cross Clackamas River.
29.4	Take Exit 9 "Downtown Oregon City."
29.7	Turn left onto McLoughlin Boulevard, OR 99E. Stay in left lane.
29.8	Left turn onto 14th Street.
30.2	Turn right onto Washington Street. Bluffs on both sides of Willamette River ahead are Columbia River Basalt flows.
30.8	Left at blinking traffic light onto 5th Street. In one block, turn right onto Adams Street.
31.1	Park in lot on right and hike up abandoned Waterboard Park Road to overgrown quarry.

Stop 8: Quarry in Waterboard Park, Oregon City. Basalt of Canemah (45.34922°N, 122.60873°W)

The quarry was developed in a bluff marking the distal end of the basalt of Canemah (Fig. 3), a widespread flow complex that issued from a vent located ~12 km to the southeast and flowed westward to the ancestral Willamette River (I.P. Madin, 2004, written commun.). The flow above the pile of large talus blocks (probably owing to undercutting by the Missoula Floods)

Figure 10. Section of cinder cone at Mount Tabor Park (Stop 6). Outcrop is ~6 m high.

is relatively thick and exhibits crude columnar to blocky jointing (Fig. 11); it probably represents lava that ponded in a stream valley or similar depression. A short distance farther along the road are roadcuts in thin flow lobes with vesicular upper and lower flow breccias. Canemah flows are LKT similar to the Mount Scott lavas. (Table 1, #9). They are magnetically reversed (Fig. 6) and were emplaced during a relatively brief eruptive episode at ca. 2.5 Ma that initiated volcanism in the Boring Volcanic Field.

End of road log. Retrace route back to I-205 and return to Oregon Convention Center via I-84.

ACKNOWLEDGMENTS

Ray Wells instigated our examination of the Boring Volcanic Field and has patiently continued to support the seemingly unending field and laboratory work it has entailed. Ian Madin and the late Marv Beeson contributed their extensive knowledge of western Oregon geology as well as samples and detailed geologic mapping. Allison Duvall, Philip Dinterman, and Michael Sawlan are responsible for integrating the large amount of information obtained by somewhat technophobic geologists into a coherent GIS database. Many landowners generously allowed access to private property. Todd Parker and Angela Crawford (U.S. Forest Service) provided access to restricted Bull Run watershed lands. Sample preparation for chemistry and dating was accomplished in laboratories managed by Rick Bishop and Judy Fierstein. Chemical analyses were performed in the GeoAnalytical Laboratory at Washington State University, under direction of Diane Johnson-Cornelius. The long-term encouragement and insights into the significance of Boring volcanism by William Leeman is particularly appreciated. We thank Julie Donnelly-Nolan and Martin Streck for their timely and valuable technical reviews.

REFERENCES CITED

Allen, J.E., 1957, Columbia River Gorge: Portland to The Dalles, *in* Guidebook for Field Trip Excursions: Geological Society of America Cordilleran Section: Eugene, Oregon, University of Oregon, p. 4–23.

Allen, J.E., 1975, Volcanoes of the Portland area: Ore Bin, v. 37, p. 145–157.

Bacon, C.R., Bruggman, P.E., Christiansen, R.L., Clynne, M.A., Donnelly-Nolan, J.M., and Hildreth, W., 1997, Primitive magmas at five Cascades volcanic fields: melts from hot, heterogeneous sub-arc mantle: Canadian Mineralogist, v. 35, p. 397–423.

Barnes, M.L., 1995, Geochemistry of the Boring Lava along the west side of the Tualatin Mountains and of sediments from drill holes in the Portland and Tualatin Basins, Portland, Oregon [M.S. thesis]: Portland, Oregon, Portland State University, 182 p.

Benito, G., and O'Connor, J.E., 2003, Number and size of last-glacial Missoula floods in the Columbia River valley between the Pasco Basin, Washington and Portland, Oregon: Geological Society of America Bulletin, v. 115, p. 624–638, doi: 10.1130/0016-7606(2003)115<0624:NASOLM>2.0.CO;2.

Blackwell, D.D., Steele, J.L., Frohme, M.K., Murphey, C.F., Priest, G.R., and Black, G.L., 1990a, Heat flow in the Oregon Cascade Range and its correlation with regional gravity, Curie point depths, and geology: Journal of Geophysical Research, v. 95, p. 19,475–19,493, doi: 10.1029/JB095iB12p19475.

Blackwell, D.D., Steele, J.L., and Kelley, S., 1990b, Heat flow in the State of Washington and thermal conditions in the Cascade Range: Journal of Geophysical Research, v. 95, p. 19,495–19,516, doi: 10.1029/JB095iB12p19495.

Blakely, R.J., Wells, R.E., Yelin, T.S., Madin, I.P., and Beeson, M.H., 1995, Tectonic setting of the Portland-Vancouver area, Oregon and Washington—Constraints from low-altitude aeromagnetic data: Geological Society of America Bulletin, v. 107, p. 1051–1062, doi: 10.1130/0016-7606(1995)107<1051:TSOTPV>2.3.CO;2.

Blakely, R.J., Wells, R.E., Tolan, T.L., Beeson, M.H., Trehu, A.M., and Liberty, L.M., 2000, New aeromagnetic data reveal large strike-slip(?) faults in the northern Willamette Valley, Oregon: Geological Society of America Bulletin, v. 112, p. 1225–1233, doi: 10.1130/0016-7606(2000)112<1225:NADRLS>2.3.CO;2.

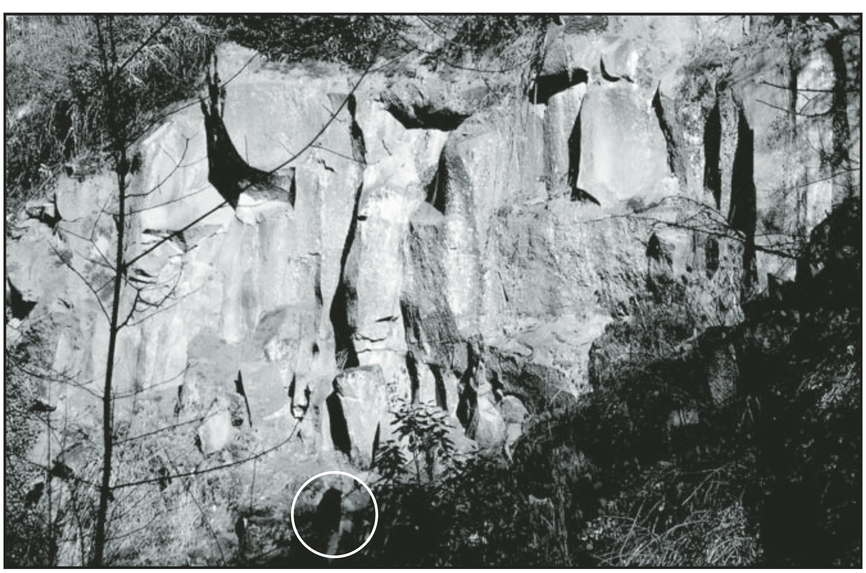

Figure 11. Blocky-columnar basalt of Canemah flow (low-K tholeiite) at Waterboard Park, Oregon City (Stop 8). Person at base of cliff (circle) for scale.

Blakely, R.J., Brocher, T.M., and Wells, R.E., 2005, Subduction-zone magnetic anomalies and implications for hydrated forearc mantle: Geology, v. 33, p. 445–448, doi: 10.1130/G21447.1.

Bostock, M.G., Hyndman, R.D., Rondenay, S., and Peacock, S.M., 2002, An inverted continental Moho and serpentinization of the forearc mantle: Nature, v. 417, p. 536–540, doi: 10.1038/417536a.

Connor, C.B., and Conway, F.M., 2000, Basaltic volcanic fields, *in* Sigurdsson, H., ed., Encyclopedia of Volcanoes: Academic Press, p. 331–343.

Conrey, R.M., Uto, K., Uchiumi, S., Beeson, M.H., Madin, I.P., Tolan, T.L., and Swanson, D.A., 1996a, Potassium-argon ages of Boring Lava, northwest Oregon and southwest Washington: Isochron-West, no. 63, p. 3–9.

Conrey, R.M., Sherrod, D.R., Uto, K., and Uchiumi, S., 1996b, Potassium-argon ages from Mount Hood area of Cascade Range, northern Oregon: Isochron-West, no. 63, p. 10–20.

Conrey, R.M., Sherrod, D.R., Hooper, P.R., and Swanson, D.A., 1997, Diverse primitive magmas in the Cascade Arc, northern Oregon and southern Washington: Canadian Mineralogist, v. 35, p. 367–396.

Conrey, R.M., Grunder, A., and Schmidt, M., 2004, State of the Cascade Arc: stratovolcano persistence, mafic lava shields, and pyroclastic volcanism associated with intra-arc rift propagation: Oregon Department of Geology and Mineral Industries Open File Report O-04-04, 39 p.

Conrey, R.M., Evarts, R.C., Leeman, W.P., Streck, M.J., Smith, R., and Fleck, R.J., 2007, A petrologic overview of the Boring volcanic field, Cascade Range, USA: Geological Society of America Abstracts with Programs, v. 39, no. 4, p. 29.

Darton, N.H., 1909, Structural materials in parts of Oregon and Washington: U.S. Geological Survey Bulletin 387, 33 p.

Evarts, R.C., and O'Connor, J.E., 2008, Geologic map of the Camas quadrangle, Clark County, Washington, and Multnomah County, Oregon: U.S. Geological Survey Scientific Investigations Map 3017, scale 1:24,000, http://pubs.usgs.gov/sim/3017.

Fleck, R.J., Sutter, J.F., and Elliot, D.H., 1977, Interpretation of discordant $^{40}Ar/^{39}Ar$ age-spectra from Antarctica: Geochimica et Cosmochimica Acta, v. 41, p. 15–32, doi: 10.1016/0016-7037(77)90184-3.

Fisher, R., 1953, Dispersion on a sphere: Proceedings of the Royal Society of London, v. A217, p. 295–305.

Flück, P., Hyndman, R.D., and Wang, K., 1997, Three-dimensional dislocation model for great earthquakes of the Cascadia subduction zone: Journal of Geophysical Research, v. 102, p. 20,539–20,550, doi: 10.1029/97JB01642.

Grove, T.L., Baker, M.B., Price, R.C., Parman, S.W., Elkins-Tanton, L.T., Chatterjee, N., and Müntener, O., 2005, Magnesian andesite and dacite lavas from Mt. Shasta, northern California: products of fractional crystallization of H_2O-rich mantle melts: Contributions to Mineralogy and Petrology, v. 148, p. 542–565, doi: 10.1007/s00410-004-0619-6.

Guffanti, M., and Weaver, C.S., 1988, Distribution of Late Cenozoic volcanic vents in the Cascade Range: Volcanic arc segmentation and regional tectonic considerations: Journal of Geophysical Research, v. 93, p. 6513–6529, doi: 10.1029/JB093iB06p06513.

Hacker, B.R., Abers, G.A., and Peacock, S.M., 2003, Subduction factory: 1. Theoretical mineralogy, densities, seismic wave speeds, and H_2O contents: Journal of Geophysical Research, v. 108, p. 2029–2055, doi: 10.1029/2001JB001127.

Hammond, P.E., 1980, Reconnaissance geologic map and cross sections of southern Washington Cascade Range, latitude 45°30′–47°15′ N., longitude 120°45′–122°22.5′ W.: Portland, Oregon, Portland State University Department of Earth Sciences, scale 1:125,000, 31 p. text.

Hammond, P.E., and Korosec, M.A., 1983, Geochemical analyses, age dates, and flow-volume estimates for Quaternary volcanic rocks, southern Cascade Mountains, Washington: Washington Division of Geology and Earth Resources Open-File Report 83-13, 36 p.

Hildreth, W., 2007, Quaternary magmatism in the cascades—a geologic perspective: U.S. Geological Survey Professional Paper 1744, 125 p.

Jicha, B.R., Hart, G.L., Johnson, C.M., Hildreth, W., Beard, B.L., Shirey, S.B., and Valley, J.W., 2009, Isotopic and trace element constraints on the petrogenesis of lavas from the Mount Adams volcanic field, Washington: Contributions to Mineralogy and Petrology, v. 157, p. 189–207, doi: 10.1007/s00410-008-0329-6.

Johnson, D.M., Hooper, P.R., and Conrey, R.M., 1999, XRF analysis of rocks and minerals for major and trace elements on a single low dilution Li-tetraborate fused bead: Advances in X-ray Analysis, v. 41, p. 843–867.

Leeman, W.P., Smith, D.R., Hildreth, W., Palacz, Z.A., and Rogers, N.W., 1990, Compositional diversity of late Cenozoic basalts in a transect across the southern Washington Cascades; implications for subduction zone magmatism: Journal of Geophysical Research, v. 95, p. 19,561–19,582, doi: 10.1029/JB095iB12p19561.

Leeman, W.P., Tonarini, S., Chan, L.H., and Borg, L.E., 2004, Boron and lithium isotopic variations in a hot subduction zone; the southern Washington Cascades: Chemical Geology, v. 212, p. 101–124, doi: 10.1016/j.chemgeo.2004.08.010.

Leeman, W.P., Lewis, J.F., Evarts, R.C., Conrey, R.M., and Streck, M.J., 2005, Petrologic constraints on the thermal structure of the Cascades arc: Journal of Volcanology and Geothermal Research, v. 140, p. 67–105, doi: 10.1016/j.jvolgeores.2004.07.016.

Le Maitre, R.W., 2002, Igneous rocks—A classification and glossary of terms, (2nd ed.): Cambridge University Press, 236 p.

Madin, I.P., 1994, Geologic map of the Damascus quadrangle, Clackamas and Multnomah Counties, Oregon: Oregon Department of Geology and Mineral Industries Geological Map GMS-60, scale 1:24,000.

McCaffrey, R., Qamar, A.I., King, R.W., Wells, R.E., Khazaradze, G., Williams, C.A., Stevens, C., Vollick, J.J., and Zwick, P.C., 2007, Fault locking, block rotation and crustal deformation in the Pacific Northwest: Geophysical Journal International, v. 169, p. 1315–1340, doi: 10.1111/j.1365-246X.2007.03371.x.

Madsen, J.K., Thorkelson, D.J., Friedman, R.M., and Marshall, D.D., 2006, Cenozoic to Recent plate configurations in the Pacific Basin: Ridge subduction and slab window magmatism in western North America: Geosphere, v. 2, p. 11–34, doi: 10.1130/GES00020.1.

McCrory, P.A., Blair, J.L., Oppenheimer, D.H., and Walter, S.R., 2005, Depth to the Juan de Fuca Slab Beneath the Cascadia Subduction Margin—A 3-D Model for Sorting Earthquakes: U.S. Geological Survey Data Series 91.

McIntyre, G.A., Brooks, C., Compston, W., and Turek, A., 1966, The statistical assessment of Rb-Sr isochrons: Journal of Geophysical Research, v. 71, p. 5459–5468.

Michaelson, C.A., and Weaver, C.S., 1986, Upper mantle structure from teleseismic *P* wave arrivals in Washington and northern Oregon: Journal of Geophysical Research, v. 91, p. 2077–2094, doi: 10.1029/JB091iB02p02077.

Peck, D.L., Griggs, A.B., Schlicker, H.G., Wells, F.G., and Dole, H.M., 1964, Geology of the central and northern parts of the western Cascade Range in Oregon: U.S. Geological Survey Professional Paper 449, 56 p., scale 1:250,000.

Smith, R.S., 2008, The making of fore-arc andesite of the Portland Basin: implications for the fate of diverse primitive mantle inputs [M.S. thesis]: Portland, Oregon, Portland State University, 235 p.

Smith, R.S., Streck, M.J., and Nelson, B.K., 2006, The making of fore-arc andesite of the Portland Basin, Oregon: Eos (Transactions, American Geophysical Union), v. 87, p. 52.

Snyder, S.L., Felger, T.J., Blakely, R.J., and Wells, R.E., 1993, Aeromagnetic map of the Portland-Vancouver metropolitan area, Oregon and Washington: U.S. Geological Survey Open-File Report 93-211, scale 1:100,000.

Swanson, R.D., 1986, A stratigraphic-geochemical study of the Troutdale Formation and Sandy River Mudstone in the Portland basin and lower Columbia River Gorge [M.S. thesis]: Portland, Oregon, Portland State University, 103 p.

Tolan, T.L., and Beeson, M.H., 1984, Intracanyon flows of the Columbia River Basalt group in the lower Columbia River Gorge and their relationship to the Troutdale Formation: Geological Society of America Bulletin, v. 95, p. 463–477, doi: 10.1130/0016-7606(1984)95<463:IFOTCR>2.0.CO;2.

Tolan, T.L., Reidel, S.P., Beeson, M.H., Anderson, J.L., Fecht, K.R., and Swanson, D.A., 1989, Revisions to the estimates of the areal extent and volume of the Columbia River Basalt Group, *in* Reidel, S.P., and Hooper, P.R., eds., Volcanism and tectonism in the Columbia River flood-basalt province: Geological Society of America Special Paper 239, p. 1–20.

Treasher, R.C., 1942a, Geologic history of the Portland area: Oregon Department of Geology and Mineral Industries Short Paper No. 7, 17 p.

Treasher, R.C., 1942b, Geologic map of the Portland area: Oregon Department of Geology and Mineral Industries Geologic Map Series GMS-7, scale 1:96,000.

Trimble, D.E., 1963, Geology of Portland, Oregon and adjacent areas: U.S. Geological Survey Bulletin 1119, 119 p., scale 1:62,500.

Van Keken, P.E., Kiefer, B., and Peacock, S.M., 2002, High-resolution models of subduction zones: implications for mineral dehydration reactions and transport of water into the deep mantle: Geochemistry Geophysics Geosystems, v. 3, p. 1056–1075, doi: 10.1029/2001GC000256.

Waitt, R.B., Jr., 1994, Scores of gigantic, successively smaller Lake Missoula floods through channeled scabland and Columbia valley, *in* Swanson, D.A., and Haugerud, R.A., eds., Geologic field trips in the Pacific Northwest: Seattle, University of Washington Department of Geological Sciences, p. 1K1–1K88.

Waitt, R.B., Jr., 1996, Numerous colossal Missoula Floods through Columbia Gorge and Portland-Vancouver basin: Geological Society of America Abstracts with Programs, v. 28, no. 5, p. 120–121.

Waters, A.C., 1973, The Columbia River Gorge—Basalt stratigraphy, ancient lava dams, and landslide dams, *in* Beaulieu, J.D., ed., Geologic field trips in northern Oregon and southern Washington: Oregon Department of Geology and Mineral Industries Bulletin 77, p. 133–162.

Wells, R.E., Weaver, C.S., and Blakely, R.J., 1998, Fore-arc migration in Cascadia and its neotectonic significance: Geology, v. 26, p. 759–762, doi: 10.1130/0091-7613(1998)026<0759:FAMICA>2.3.CO;2.

Wells, R.E., Niem, A.R., Evarts, R.C., and Hagstrum, J.T., 2009, this volume, The Columbia River Basalt Group—From the gorge to the sea, *in* O'Connor, J.E., Dorsey, R.J., and Madin, I.P., eds., Volcanoes to Vineyards: Geologic Field Trips through the Dynamic Landscape of the Pacific Northwest: Geological Society of America Field Guide 15, doi: 10.1130/2009.fld015(32).

White, J.D.L., 1991, The depositional record of small, monogenetic volcanoes within terrestrial basins, *in* Fisher, R.V., and Smith, G.A., eds., Sedimentation in volcanic settings: SEPM Special Publication 45, p. 155–171.

Williams, I.A., 1916, The Columbia River Gorge—its geologic history interpreted from the Columbia River Highway: Oregon Bureau of Mines and Geology, Mineral Resources of Oregon, v. 2, no. 3, rev. 1923, 130 p. (reprinted by Oregon Historical Society, 1991).

Wilson, D.S., 1988, Tectonic history of the Juan de Fuca Ridge over the last 40 million years: Journal of Geophysical Research, v. 93, p. 11,863–11,876, doi: 10.1029/JB093iB10p11863.

Wilson, D.S., 2002, The Juan de Fuca plate and slab: Isochron structure and Cenozoic plate motions, *in* Kirby, S., Wang, K., and Dunlop, S., eds., The Cascadia subduction zone and related subduction systems: U.S. Geological Survey Open-File Report 02-328, p. 9–12.

Wood, C.A., 1980, Morphometric analysis of cinder cone degradation: Journal of Volcanology and Geothermal Research, v. 8, p. 137–160, doi: 10.1016/0377-0273(80)90101-8.

Yelin, T.S., and Patton, H.J., 1991, Seismotectonics of the Portland, Oregon, region: Bulletin of the Seismological Society of America, v. 81, p. 109–130.

Manuscript Accepted by the Society 29 June 2009

Printed in the USA